

Submonolayer InGaAs/GaAs quantum-dot lasers with high modal gain and zero-linewidth enhancement factor

Xu, Zhangcheng; Birkedal, Dan; Juhl, Michael; Hvam, Jørn Marcher

Published in:
Applied Physics Letters

Link to article, DOI:
[10.1063/1.1806564](https://doi.org/10.1063/1.1806564)

Publication date:
2004

Document Version
Publisher's PDF, also known as Version of record

[Link back to DTU Orbit](#)

Citation (APA):
Xu, Z., Birkedal, D., Juhl, M., & Hvam, J. M. (2004). Submonolayer InGaAs/GaAs quantum-dot lasers with high modal gain and zero-linewidth enhancement factor. *Applied Physics Letters*, 85(15), 3259-3261. DOI: 10.1063/1.1806564

DTU Library

Technical Information Center of Denmark

General rights

Copyright and moral rights for the publications made accessible in the public portal are retained by the authors and/or other copyright owners and it is a condition of accessing publications that users recognise and abide by the legal requirements associated with these rights.

- Users may download and print one copy of any publication from the public portal for the purpose of private study or research.
- You may not further distribute the material or use it for any profit-making activity or commercial gain
- You may freely distribute the URL identifying the publication in the public portal

If you believe that this document breaches copyright please contact us providing details, and we will remove access to the work immediately and investigate your claim.

Submonolayer InGaAs/GaAs quantum-dot lasers with high modal gain and zero-linewidth enhancement factor

Zhangcheng Xu^{a)}

The Key Lab of Advanced Technique and Fabrication for Weak-Light Nonlinear Photonics Materials, Ministry of Education, Nankai University, Tianjin 300071, P.R. China and Research Center COM, Technical University of Denmark, DK-2800, Lyngby, Denmark

Dan Birkedal, Michael Juhl, and Jørn M. Hvam

Research Center COM, Technical University of Denmark, DK-2800, Lyngby, Denmark

(Received 17 May 2004; accepted 17 August 2004)

The gain spectra of a submonolayer (SML) InGaAs/GaAs quantum dot (QD) laser working at 30 °C were measured using the Hakki–Paoli method. It is found that the maximum modal gain of QD ground states is as high as 44 cm⁻¹ and no gain saturation occurs below the threshold at the lasing wavelength of 964.1 nm. When the injection current is about 0.98 times the threshold, the gain spectrum becomes symmetric with respect to the lasing wavelength, and zero-linewidth enhancement factor is observed. These properties are attributed to the high density and the high uniformity of SML QDs in our laser diode. © 2004 American Institute of Physics.

[DOI: 10.1063/1.1806564]

As an alternative growth mode to the conventional Stranski–Krastanow (SK) mode of growing self-assembled semiconductor quantum dots (QDs), submonolayer (SML) deposition has recently received some attention, due to its potential of fabricating QDs with high density and high uniformity.^{1–3} The deposition of a short-period InAs/GaAs superlattice on a GaAs (100) surface, with an InAs effective thickness of less than 1 monolayer (ML) and a suitable number of periods, results in the formation of nanometer scale (In, Ga) As QDs of a non-SK class.⁴ Recently, an SML InGaAs/GaAs QD heterostructure is verified to be a QD quantum-well (QW) structure, i.e., the indium-rich QDs are embedded in a lateral quantum well (QW) with lower indium content.^{5,6} High-power lasers with SML InGaAs/GaAs QDs as the active region have been demonstrated.^{4,7,8} Although the gain properties of SK InGaAs/GaAs QD lasers have been studied intensively,^{9–17} the gain properties of SML InGaAs/GaAs QD lasers have not been reported. In this letter, we report the measurement of the gain spectra and the determination of the linewidth enhancement factor of an SML InGaAs/GaAs QD laser.

The epitaxial structure was grown by solid-source molecular-beam epitaxy on an *n*⁺-doped GaAs (100) substrate. It consists of an *n*-type (10¹⁸ cm⁻³) 0.5 μm thick GaAs buffer, a 1.5 μm thick *n*-type (10¹⁸ cm⁻³) Al_{0.2}Ga_{0.8}As lower cladding layer, 200 nm thick GaAs confining layers (*n* = 10¹⁷ cm⁻³ and *p* = 10¹⁷ cm⁻³) surrounding the laser active region, a 1.5 μm *p*-type (10¹⁸ cm⁻³) upper cladding layer, and a *p*⁺-doped (10¹⁹ cm⁻³) 200 nm thick GaAs cap for ohmic contact. In the active region, 0.5 ML InAs and 2.5 ML GaAs were alternately deposited at 500 °C with 10 periods, to form the SML QD layer. All the other layers were grown at 600 °C. A photoluminescence signal from the QD ground states is still observable at room temperature, for an SML InGaAs/GaAs QD sample grown under the same conditions as the QDs in the laser structure. A broad-area edge-emitting SML InGaAs/GaAs QD laser with a 100 μm wide

stripe, a 628 μm long cavity and uncoated facets, was fabricated and mounted with the *n*-side down on a thermoelectric cooler. The emitted light is dispersed by a high-resolution spectrometer and detected by a Si charge-coupled-device. Far-field spatial filtering is employed to remove the interference of a large number of lateral modes.¹⁸ Measurements were performed at 30 °C, under pulsed excitation to eliminate additional heating. The pulse width is 0.2 μs, and the duty cycle is 0.1%.

The gain spectrum is measured using the Hakki–Paoli method.¹⁹ The difference between the modal gain g_{mod} and the internal loss α_i , i.e., the net modal gain $g_{\text{net}} = g_{\text{mod}} - \alpha_i$, is given by

$$g_{\text{net}} = \frac{1}{L} \ln \left(\frac{r^{1/2} - 1}{r^{1/2} + 1} \right) - \frac{1}{2L} \ln(R_1 R_2), \quad (1)$$

where L is the cavity length, R_1 and R_2 are the power reflectivity of the cleaved facets, and r is the peak-to-valley ratio

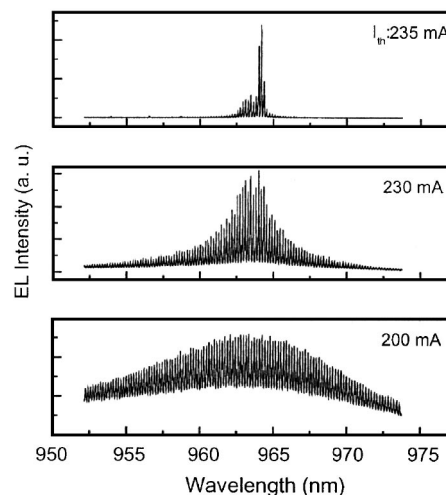


FIG. 1. The electroluminescence spectra measured from the side of an SML InGaAs/GaAs QD laser, at 30 °C. The threshold current is 235 mA, and the lasing wavelength is 964.1 nm.

^{a)}Electronic mail: zcxu@nankai.edu.cn

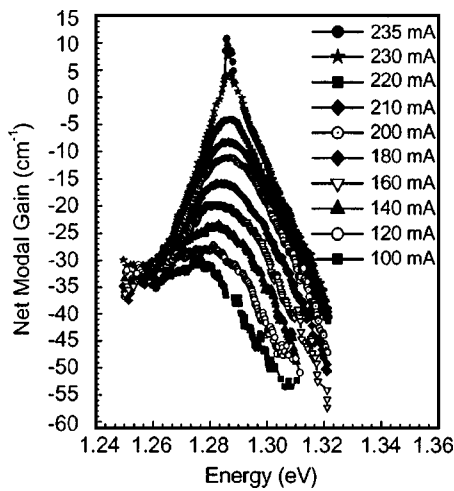


FIG. 2. Net modal gain spectra of an SML InGaAs/GaAs QD laser at different injection currents.

of the Fabry–Perot oscillations in the intensity of the light emitted from the device. In the long-wavelength limit, g_{mod} approaches zero, therefore, the measured g_{net} will be equal to $-\alpha_i$ from which the spectrum of the modal gain can be obtained.²⁰ Figure 1 shows the typical emission spectra at 200 mA, 230 mA, and 235 mA (I_{th}). Figure 2 shows the net modal gain spectra at several currents. The mirror reflectivity is assumed to be 0.35, corresponding to a mirror loss α_m of 16.7 cm^{-1} . It can be seen from Fig. 2, that the maximum of the gain spectrum curve moves toward higher photon energies with increasing injection current. As this takes place, the shape of gain spectrum becomes more symmetric near its maximum. When the current is 230 mA, just below the threshold, the half-width of the gain spectrum is about 26.7 meV. This value is two to three times narrower than that of typical SK InAs/GaAs QD lasers reported in Ref. 21. The narrower gain spectrum is due to higher uniformity of the QD arrays in our device.

At the low-energy limit (1.25 eV), the spectra converge ($g_{\text{net}} = -33 \pm 2 \text{ cm}^{-1}$), therefore, the internal loss should be about 33 cm^{-1} .²⁰ At the lasing threshold, the maximum net modal gain is measured to be $11 \pm 1 \text{ cm}^{-1}$, corresponding to a maximum modal gain of about $44 \pm 3 \text{ cm}^{-1}$. The maximum modal gain of QD ground states for a single sheet of SK InGaAs/GaAs QDs has been reported to be between $(11 \pm 4) \text{ cm}^{-1}$ and 33.8 cm^{-1} in Refs. 9–15. Thus, our result represents, a very high value of the modal gain from the ground states of a single sheet of self-assembled QDs.

Another important parameter of semiconductor lasers is the linewidth enhancement factor (α -factor). In high-power

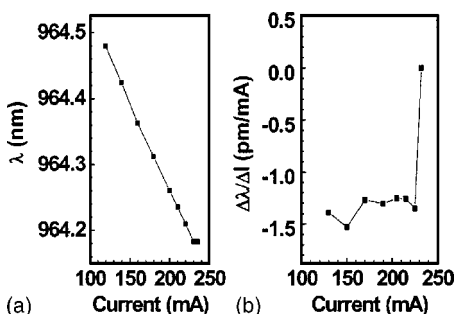


FIG. 3. Wavelength (a) and its shift (b) vs current for the lasing mode.

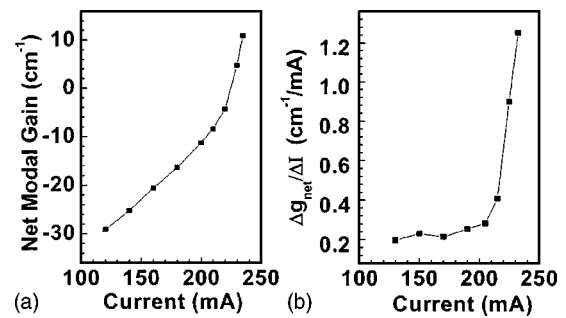


FIG. 4. Net modal gain (a) and differential gain (b) vs current at lasing wavelength.

semiconductor laser applications, the α -factor must be minimized in order to reduce filamentation effect. The α -factor can be found from the relation²²

$$\alpha \approx -\frac{2\pi}{\delta\lambda \cdot L} \cdot \frac{\Delta\lambda/\Delta I}{\Delta g_{\text{net}}/\Delta I}, \quad (2)$$

where $\delta\lambda$ is the Fabry–Perot mode spacing, L is the cavity length, $\Delta\lambda/\Delta I$ is the mode wavelength shift with current (equivalent to the change in refractive index with pumping current), and $\Delta g_{\text{net}}/\Delta I$ is the change in net modal gain with current. Figure 3 shows the wavelength λ and the shift $\Delta\lambda/\Delta I$ as a function of current, for the lasing mode. In Fig. 3(b), the abscissa of the graph markers is placed at the average of the two current levels used from Fig. 3(a). As the current increases, the wavelength blueshifts at a constant rate $\Delta\lambda/\Delta I \cong 1.5 \times 10^{-3} \text{ nm/mA}$ for currents below $0.98I_{\text{th}}$, and then almost stays constant, resulting in a drastic decrease of $|\Delta\lambda/\Delta I|$, which is nearly zero from $0.98I_{\text{th}}$ to $0.10I_{\text{th}}$. Figure 4 shows the net modal gain and the differential gain $\Delta g_{\text{net}}/\Delta I$ as a function of current at the lasing wavelength. The net modal gain increases linearly with the increase of current when the current is below $0.91I_{\text{th}}$, and superlinearly above. Correspondingly, $\Delta g_{\text{net}}/\Delta I$ is almost a constant below $0.91I_{\text{th}}$, and then increases significantly. These trends are in contrast to the current dependence of differential gain in similar-design InGaAs/GaAs QW lasers, which was presented in Ref. 23. In QW lasers, the differential gain was found to be the highest at low current density, gradually decreasing with increasing the carrier density as the states associated with the $n=1$ transition fill. In addition, no saturation of the gain and the differential gain is observed below I_{th} in our SML-grown QD lasers, while saturation is very pronounced for typical SK-grown QD lasers,^{16,17} when the current is near to the threshold.

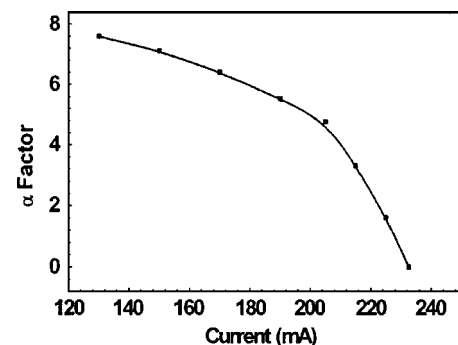


FIG. 5. Linewidth enhancement factor at the lasing wavelength as a function of current, for an SML InGaAs/GaAs QD laser.

With the data in Figs. 3(b) and 4(b), the α -factor is determined as a function of current for the lasing mode, as shown in Fig. 5. It can be seen that the α -factor decreases to zero when the current increases to $0.98I_{th}$. This is our first observation of a zero linewidth enhancement factor at the lasing wavelength for QD lasers. When the current is very near to the threshold, the carrier–carrier scattering (Auger process) will be the dominant mechanism of carrier capture and relaxation,²⁴ and the population probability for all the QDs is almost the same, resulting in a very symmetric gain spectrum. In this case, the differential gain is also symmetric to the peak gain energy position where lasing occurs. Thus, the change of the differential refractive index computed via the Kramers–Kronig relation is exactly zero at the lasing energy (i.e., the peak gain position). For SK QD lasers with a single sheet of QDs, the ground states of QDs can be easily saturated due to the lower density of QDs. The contribution of excited states or wetting-layer states to the gain might cause an asymmetric gain curve, which increases the linewidth enhancement, depending on excitation level, to about 0.5 in Ref. 25, 0.1 in Ref. 17, 0.15 in Ref. 16, or 0.7 in Ref. 26. Our observation of zero-linewidth enhancement factor at the lasing wavelength is attributed to the high density of SML QDs in our devices.

In summary, we have observed a narrow gain spectrum, high modal gain, the increasing differential gain, and zero-linewidth enhancement factor in an SML InGaAs/GaAs QD laser diode. These properties are attributed to the high density and the high uniformity of SML QDs in our devices and they are very promising for the application of SML QDs in high-power lasers.

This work was supported by the Danish Technical Science Research Council.

¹I. L. Krestnikov, N. N. Ledentsov, A. Hoffmann, and D. Bimberg, *Phys. Status Solidi A* **183**, 207 (2001).

²N. N. Ledentsov and D. Bimberg, *J. Cryst. Growth* **255**, 68 (2003).

³V. Bressler-Hill, A. Lorke, S. Varma, P. M. Petroff, K. Pond, and W. H. Weinberg, *Phys. Rev. B* **50**, 8479 (1994).

⁴S. S. Mikhlin, A. E. Zhukov, A. R. Kovsh, N. A. Marleev, V. M. Ustinov, Y. M. Shernyakov, I. P. Soshnikov, D. A. Livshits, I. S. Tarasov, D. A. Bedarev, B. V. Volovik, M. V. Maximov, A. F. Tsatsulnikov, N. N. Ledentsov, P. S. Kopev, D. Bimberg, and Z. I. Alferov, *Semicond. Sci. Technol.* **15**, 1061 (2000).

⁵Z. C. Xu, D. Birkedal, J. M. Hvam, Z. Y. Zhao, Y. M. Liu, K. T. Yang, A. Kanjilal, and J. Sadowski, *Appl. Phys. Lett.* **82**, 3859 (2003).

⁶Z. C. Xu, K. Leosson, D. Birkedal, V. Lyssenko, J. M. Hvam, and J. Sadowski, *Nanotechnology* **14**, 1259 (2003).

⁷A. F. Zhukov, A. R. Kovsh, S. S. Mikhlin, N. A. Maleev, V. M. Ustinov, D. A. Livshits, I. S. Tarasov, D. A. Bedarev, M. V. Maximov, A. F. Tsatsulnikov, I. P. Soshnikov, P. S. Kopev, Z. I. Alferov, N. N. Ledentsov, and D. Bimberg, *Electron. Lett.* **35**, 1845 (1999).

⁸A. R. Kovsh, A. E. Zhukov, N. A. Maleev, S. S. Mikhlin, D. A. Livshits, Y. M. Shernyakov, M. V. Maximov, N. A. Pihiti, I. S. Tarasov, V. M. Ustinov, Z. I. Alferov, J. S. Wang, L. Wei, G. Lin, J. Y. Chi, N. N. Ledentsov, and D. Bimberg, *Microelectron. J.* **34**, 491 (2003).

⁹E. Herrman, P. M. Smowton, H. D. Summers, J. D. Thomson, and M. Hopkinson, *Appl. Phys. Lett.* **77**, 163 (2000).

¹⁰P. M. Smowton, E. Herrmann, Y. Ning, H. D. Summers, and P. Blood, *Appl. Phys. Lett.* **78**, 2629 (2001).

¹¹F. Y. Chang, C. C. Wu, and H. H. Lin, *Appl. Phys. Lett.* **82**, 4477 (2003).

¹²P. G. Eliseev, H. Li, A. Stintz, G. T. Liu, T. C. Newell, K. J. Malloy, and L. F. Lester, *Appl. Phys. Lett.* **77**, 262 (2000).

¹³S. Bogna, M. Grundmann, O. Stier, D. Ouyang, C. Ribbat, R. Heitz, R. Sellin, and D. Bimberg, *Phys. Status Solidi B* **224**, 823 (2001).

¹⁴A. E. Zhukov, A. R. Kovsh, S. S. Mikhlin, A. P. Vasil'ev, E. S. Semenova, N. A. Maleev, V. M. Ustinov, M. M. Kulagin, E. V. Nikitin, I. P. Soshnikov, Yu. M. Shernyakov, D. A. Livshits, N. V. Kryzhanovskaya, D. S. Sizov, M. V. Maximova, A. F. Tsatsul'nikov, N. N. Ledentsov, D. Bimberg, and Z. I. Alferov, *Physica E (Amsterdam)* **17**, 589 (2003).

¹⁵B. Sumpf, S. Deubert, G. Erbert, J. Fricke, J. P. Reithmaier, A. Forchel, R. Staske, and G. Trankle, *Electron. Lett.* **39**, 1655 (2003).

¹⁶P. K. Kondratko, S. L. Chuang, G. Walter, T. Chung, and N. Holonyak, *Appl. Phys. Lett.* **83**, 4818 (2003).

¹⁷T. C. Newell, D. J. Bossert, A. Stintz, B. Fuchs, and K. J. Molloy, *IEEE Photonics Technol. Lett.* **11**, 1527 (1999).

¹⁸D. J. Bossert and D. Gallant, *Electron. Lett.* **32**, 338 (1996).

¹⁹B. W. Hakki and T. L. Paoli, *J. Appl. Phys.* **46**, 1299 (1974).

²⁰L. Ketelse, *Electron. Lett.* **28**, 171 (1992); C. S. Chang, S. L. Chuang, J. R. Minch, W. W. Fang, Y. K. Chen, and T. Tanbun-Ek, *IEEE J. Sel. Top. Quantum Electron.* **1**, 1100 (1995).

²¹M. V. Maximov, Y. M. Shernyakov, A. F. Tsatsul'nikov, A. V. Lunev, A. V. Sakharov, V. M. Ustinov, A. Y. Egorov, A. E. Zhukov, A. R. Kovsh, P. S. Kop'ev, L. V. Asryan, Z. I. Alferov, N. N. Ledentsov, D. Bimberg, A. O. Kosogov, and P. Werner, *J. Appl. Phys.* **83**, 5561 (1998).

²²A. Schonfelder, S. Weisser, J. D. Ralston, and J. Rosenzweig, *IEEE Photonics Technol. Lett.* **6**, 891 (1994).

²³W. Rideout, B. Yu, J. LaCourse, P. K. York, K. J. Beernink, and J. J. Coleman, *Appl. Phys. Lett.* **56**, 706 (1990).

²⁴A. V. Uskov, Y. Boucher, J. Le Bihan, and J. McInerney, *Appl. Phys. Lett.* **73**, 1499 (1998).

²⁵D. Bimberg, N. Kirstaedter, N. N. Ledentsov, Z. I. Alferov, P. S. Kop'ev, and V. M. Ustinov, *IEEE J. Sel. Top. Quantum Electron.* **3**, 196 (1997).

²⁶S. Fathpour, P. Bhattacharya, S. Pradhan, and S. Ghosh, *Electron. Lett.* **39**, 1443 (2003).